

**Supplementary Material for “Direct ecosystem fluxes of
volatile organic compounds from oil palms in South-East
Asia”**

**P. K. Misztal^{1,2*}, E. Nemitz¹, B. Langford¹, C. Di Marco¹, G. J. Phillips^{1#}, C. N.
Hewitt³, R. MacKenzie³, S. M. Owen¹, D. Fowler¹, M. R. Heal² and J. N. Cape¹**

[1]{Centre for Ecology & Hydrology, Penicuik, EH26 0QB, UK}

[2]{School of Chemistry, University of Edinburgh, EH9 3JJ, UK}

[3]{Lancaster Environment Centre, Lancaster University, LA1 4YQ, UK}

* Currently at Department of Environmental Science, Policy, and Management, University of
California, Berkeley, CA, US

Now at NCAS, School of Earth and Environment, University of Leeds, UK.

Correspondence to: P.K. Misztal (pkm@berkeley.edu)

SI-1 Ambient and canopy temperature

Figure S1 shows diurnal patterns of measured ambient temperature and the average canopy
temperature estimated from extrapolation of the ambient temperature to the surface, using the
sensible heat flux and the resistance approach (Nemitz et al., 2009).

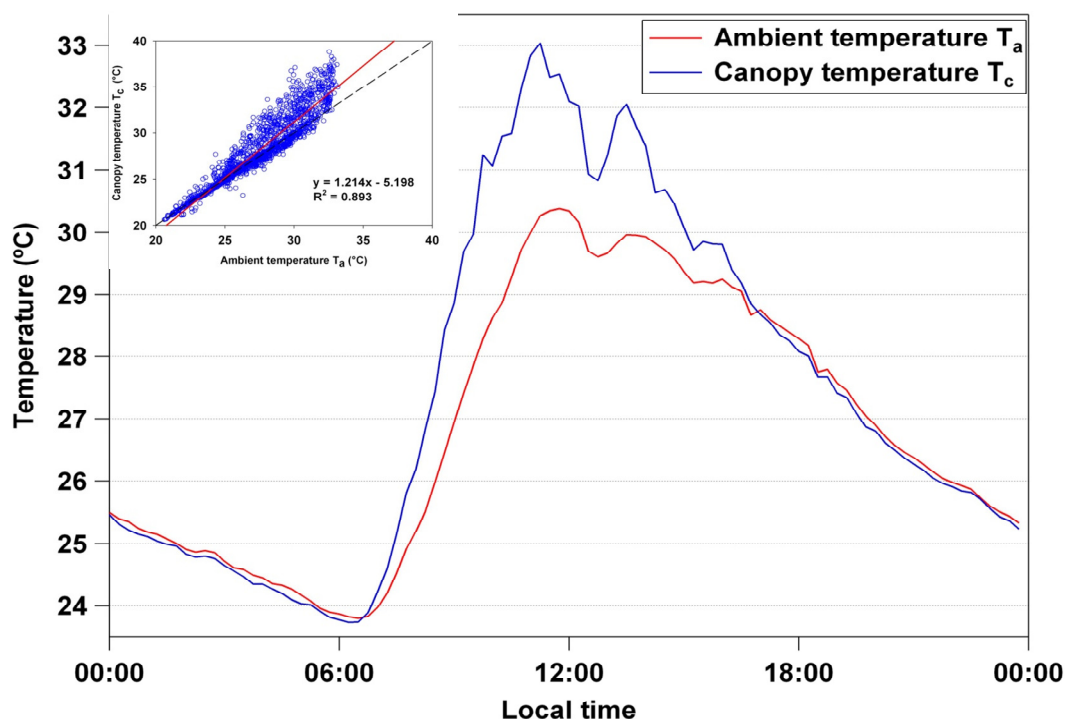


Figure S1. Comparison between the ambient (T_a (15 m)) and canopy (T_c) temperature estimated from resistance approach showing T_c higher by approximately 2 °C during the midday and lower by 0.2 °C at night. Inset shows regression and higher variability of T_c in the upper temperature range.

SI-2 Proton Transfer Reaction Mass Spectrometry (PTR-MS)

The concentrations and eddy fluxes of biogenic volatile organic compounds (BVOCs) were measured by a Proton-Transfer-Reaction Mass Spectrometer (PTR-MS) operated in continuous flow disjunct eddy covariance (cfDEC) mode, also referred to as the virtual disjunct eddy covariance (vDEC) mode, described in the next section. The instrument was the high-sensitivity model (Ionicon, Austria, s/n 04-03) which was equipped with an additional turbomolecular pump for the detection chamber and incorporated Teflon®, instead of Viton®, gaskets in the drift tube. Since the characteristics of instrument design and operation have been thoroughly described in the literature (Blake et al., 2009; de Gouw, 2007; Hansel et al., 1995; Lindinger et al., 1998; Warneke et al., 2001), only a general overview specific to running at high humidity will be given here.

The principle of PTR-MS is the soft ionisation of VOCs by hydronium ions formed in a hollow cathode ion-source from pure water vapour; these effectively transfer protons to all

1 molecules with proton affinities (PA) greater than that of water. Most VOCs have sufficiently
2 large PA for effective ion transfer, but a few low-weight molecular compounds, with PA only
3 slightly higher than water (e.g. formaldehyde), may require specific optimisation to minimise
4 the impact on sensitivity of humidity dependent back-reactions. The conditions inside the
5 reaction chamber are dependent on both electric field (E) and the number density of the buffer
6 gas (N) and the ratio of these (E/N) determines the degree of fragmentation and clustering. At
7 typical ambient conditions this ratio is kept in the range 120 – 140 Td ($1 \text{ Td} = 10^{-17} \text{ V cm}^2$).
8 However, for a constant E/N ratio the sensitivity is proportional to N and thus operation at 2
9 mbar or larger is recommended (Warneke et al., 2001). The protonated ions are filtered
10 through a quadrupole mass filter (QMA 400) and counted with a Secondary Electron
11 Multiplier (Pfeiffer SEM-217) coupled to an ion-count preamplifier (Pfeiffer CP-400). The
12 radio frequency and direct current are generated by an RF box (Pfeiffer QMH 400). Since the
13 sampled VOCs undergo protonation, they are detected at a mass to charge (m/z) ratio equal to
14 one unit greater than their molecular weight. The soft ionisation method means that most
15 compounds can be detected as their parent ion. For heavier compounds ($m/z > 100$) the
16 protonated masses reflecting two or more fragments may need to be taken into account. This
17 is the case, for example, for monoterpenes (m/z 137, 81) (e.g. Tani et al., 2003) and
18 sesquiterpenes (m/z 205, 149) (Kim et al., 2009). Because some compounds fragment more
19 than others, appropriate calibration and calculation approaches have to be applied (sections
20 SI-3 and SI-5).

21 The optimisation of the PTR-MS and the sampling system sought a compromise between
22 reliable measurements at very high humidity and sensitivity for VOCs. Tani et al. (2004)
23 showed that sample humidity has a significant impact on fragmentation patterns at normal
24 E/N ratios, but has no influence if E/N is kept around 140 Td. The water vapour pressures
25 tested by these authors ranged from 0.59 to 2.4 kPa. However, the vapour pressures
26 encountered at the oil palm site were much higher, ranging from 2.5 to 3.2 kPa (2.75 kPa on
27 average) due to high relative humidity (88% on average) accompanied by high temperatures
28 (22 – 31 °C). Humidity effects on PTR-MS measurements were also studied by Warneke et
29 al. (2001), who noted decreasing sensitivities at higher humidities, although again the levels
30 of specific humidity encountered in Borneo were not tested by these authors. Although the
31 sensitivity could be enhanced by increasing the drift tube pressure to 2 - 3 mbar this approach
32 was not possible for the conditions here, because the high flow in the sampling line and the
33 high specific humidity would have required operation at a detection pressure close to or above

the set points of the instrument. In addition, higher drift tube pressure would have increased the likelihood of internal condensation.

Therefore, the optimal operating conditions were determined experimentally to be a drift tube pressure of 1.6 mbar, inlet and drift-tube temperatures of 45 °C and drift voltage of 485 V, giving an E/N value of 140 Td. This was maintained constant throughout the experiment. Our subsequent measurements in the laboratory revealed less than 5% reduction in sensitivity when operating at 1.6 mbar drift tube pressure, compared to 2.2 mbar at the same E/N ratio. However, high ambient water vapour pressure had an additional impact on the sensitivities, and normalisation for the presence of water clusters was required (Davison et al., 2009; Tani et al., 2004). The overall reduction in sensitivity was estimated at 20% with respect to operation at temperate humidities.

The system was automated to run continuously in 3 modes: (1) m/z 21-206 scan of ambient air; (2) multiple ion detection (MID) of 11 pre-selected VOCs at 0.5 s dwell time each (0.2 s for additional m/z 21 and 37 corresponding to $\text{H}_3^{18}\text{O}^+$ and $\text{H}_3^{16}\text{O}(\text{H}_2^{16}\text{O})^+$, respectively; and (3) m/z 21-206 background measurement of humid VOC-free air. Mode 1 was set to run for the first 5 minutes of each hour, then 25 min was devoted to mode 2, then mode 3 for 5 min and again mode 2 for the remaining 25 min. The switching between modes was automated through a solenoid valve system operated from the 12 V DC power port of the PTR-MS power supply unit and managed through a QS422 sequence. The online preview and logging of volume mixing ratios and fluxes was done using the DDE feature of the Balzer sequencer communicating with a LabVIEW program which logged the sonic anemometer data together with the PTR-MS data to one file, so that each 25-min file contained 30000 rows of wind data, 210 of which also contained PTR-MS data which were synchronised in time, but not yet corrected for the lag-time associated with the residence time in the tubing (see Sect. SI-5).

Direct calibration used a VOC gas mixture supplied by Apel-Riemer Environmental Inc., USA, which contained methanol, acetaldehyde, acetone, isoprene, acetonitrile and formaldehyde, each at 1 ppmv, and d-limonene at 0.18 ppmv. The standard was diluted on site with the same zero air from a custom-built generator containing Pt/Al₂O₃ catalyst heated to 250 °C (Misztal et al., 2010), as the zero air used for mode 3. The catalyst worked efficiently for all VOCs including methanol and provided humidity similar to the ambient. It was used at the site to dilute high concentration standard into clean Tedlar® bags using new high quality gas-tight syringes; the bags were prepared freshly just before the calibration. The

calibration range was broad from 20 pptv to 500 ppbv ensuring high precision and minimizing any potential artefacts from using the Tedlar ® bags. The subsequent calibration in the lab at the same drift conditions but with much less humid air revealed that the high humidity contributed to approximately 20% lower sensitivities in the field. The standard was checked after the campaign by reference to a GC-MS calibrated with a different isoprene standard (BOC gases, UK) and a d-limonene standard prepared from a diluted (with methanol) liquid standard (Sigma Aldrich, UK) injected directly onto the column. Agreement for isoprene and monoterpenes was within 4% and 10%, respectively. The other VOCs were compared with another gas standard delivered by Apel-Riemer (at 0.5 ppm concentration per VOC) which was 2 years older and contained the same VOCs plus MVK, and other organics. The agreement was within 18%; the older standard showed 8-18% smaller concentrations for all VOCs except for acetaldehyde, which was 8% higher possibly through contributions of fragments from other organic species (e.g. MVK) that were not present in the other mixture. It has been assumed that the calibration standard was within the certified 5% standard precision for isoprene and other VOCs at the time of calibration. A larger uncertainty of 20% has been attributed to MVK sensitivity, which was not present in the calibration standard in the field, but which was inferred from the comparison of the sensitivity curves in the laboratory derived from the MVK containing standard. It was also assumed that the sensitivity for the sum of MVK+MACR is the same as for MVK only.

SI-3 Derivation of volume mixing ratios (VMRs)

The signal intensities measured as counts per second I_{mz} (cps) for each of the monitored m/z channels were first converted to normalised counts per second I_{mz} (ncps) (Davison et al., 2009) in order to compensate for fluctuations in the primary ion, water vapour and drift-tube pressure.

$$I_{mz}(ncps) = \frac{I_{mz}(cps) \times 10^6}{I_{21}(cps) \times 500 + I_{37}(cps) + I_{55}(cps)} \times \frac{P_{dnorm}}{P_d}, \quad (S1)$$

where I_{21} , I_{37} and I_{55} are the instantaneous counts (cps) of $H_3^{18}O^+$ (approximately a factor of 500 lower than $H_3^{16}O^+$), $H_3^{16}O(H_2^{16}O)^+$, and $H_3^{16}O(H_2^{16}O)_2^+$, respectively. The m/z 21 channel instead of m/z 19 was selected for monitoring the primary ions in order to prevent

detector saturation. Generally a natural $^{16}\text{O}/^{18}\text{O}$ isotope ratio of 500 is used in the calculation (Kuhn et al., 2007; Langford et al., 2009a) although the use of a slightly lower precise ratio of 487 was proposed (Taipale et al., 2008). In fact, the true ratio might differ slightly depending on the location (e.g. close to oceanic waters) and one of the purposes of normalisation is to make the results uniform for comparisons with other results, where the level of primary ions used was different. In our case the level of primary ion counts was $6.5\text{-}7.5 \times 10^6$ cps. The volume mixing ratios (χ) were obtained for each VOC as:

$$\chi_{\text{VOC}} = \frac{I_{m/z}(\text{ncps}) - I_{m/z(\text{zero})}(\text{ncps})}{S_{m/z}(\text{ncps/ppbv})} \quad (\text{S2})$$

Here, $I_{m/z(\text{zero})}(\text{ncps})$ is the background normalised count rate for the given m/z channel, and the $S_{m/z}(\text{ncps/ppbv})$ is the normalised sensitivity for a given compound. The $S_{m/z}$ for compounds present in the gas standard was obtained from the slope of a 6-point calibration line in the range 0 to 500 ppbv (0 to 90 ppbv for monoterpenes) corrected for background $I_{m/z}(\text{ncps})$.

The standard was appropriately diluted in clean Tedlar bags using VOC-free air, generated by purging ambient air through a $\text{Pt}/\text{Al}_2\text{O}_3$ catalyst heated to 200 °C. This catalyst removed most VOCs effectively, but did not significantly affect water vapour concentrations, thereby avoiding problems arising from using dry calibration gas. However, normalisation for water clusters was always performed (Eq. S1). For compounds not present in the standard, the empirical sensitivity $S'_{m/z}$ was approximated from the relative transmission curve (RTC) (Davison et al., 2009; Taipale et al., 2008). Only the sensitivities of non-fragmenting compounds which are known not to deviate significantly from the RTC (e.g. methanol, acetaldehyde, acetone, acetonitrile) were used to derive the relationship between the sensitivities and the transmission coefficients from using the reaction rate coefficients for the proton transfer reaction taken from Zhao and Zhang (2004). Since no large m/z compounds were used in calibration, the RTC approach was limited to the 21-71 range, and was extended later after comparison to the classical transmission coefficients using higher MW compounds such as xylene and camphor. The calibration error using the standard is assumed to be less than 5% while that from using reaction rate constants can be up to 100% (Steinbacher et al., 2004). However, the relative transmission approach used here can offer less than 30% relative error (Taipale et al., 2008). Table S1 summarises the actual sensitivities for compounds reported in the paper.

Table S1. Sensitivities for targeted compounds measured at oil palm. The values were derived in calibration at the site, except for the values marked with an asterisk, which were obtained using the relative transmission approach combined with calibration in the laboratory.

<i>m/z</i>	33	45	59	69	71	75	81	83	93	137	149	205
Compound	Methanol	Acetaldehyde	Acetone	Isoprene	MVK MACR	HA	MT	Hexanals	Toluene	MT	Estragole	SQT
Sensitivity (cps ppbv ⁻¹)	84.0	72.8	84.8	22.0	38.7*	98.3*	14.6	58.5	52.5*	7.2	12.0*	6.8*

SI-4 Graphical method for LODs, standard deviations and means

For the data which had lognormal distribution, common for environmental datasets, the exponent of the slope of the lognormal line on a log-probability plot corresponds to the geometrical standard deviation (and the exponential of the intercept corresponds to the geometrical mean). The geometrical LOD can be found from the exponential of the intercept (Helsel, 1990). Similarly, for normally-distributed data, the slope of the line of non-logarithmic VMR values versus normal cumulative distributions (z) corresponds to the arithmetic standard deviation and the intercept to the arithmetic mean. For compounds whose distributions turned out to be multimodal (e.g. isoprene, MVK) the graphical methods were not applicable. The LODs, standard deviations and means derived by these methods were presented in Table 1 of the main text.

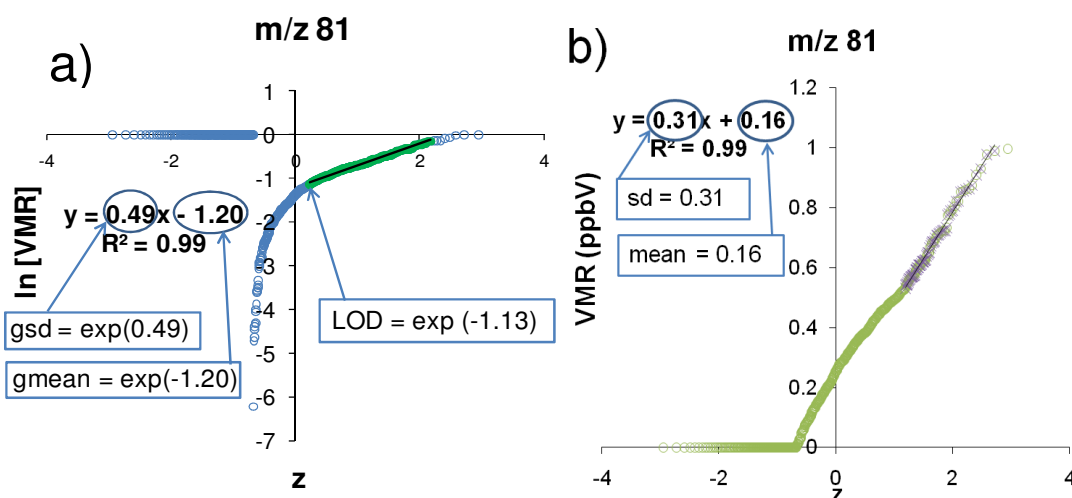


Figure S2. An example of the graphical estimation of the limit of detection and other statistical parameters from lognormal data values (a) and normal data values (b) plotted against normal cumulative distributions. Blue arrows indicate the way to derive geometrical standard deviation (gsd), geometrical mean (gmean), limit of detection (LOD), and in case of normal distribution arithmetical standard deviation (sd) and arithmetical mean (mean). Graphically derived values are compared with calculated values in Table 1 of the main text.

SI-5 Flux derivation and validation

PTR-MS, with its relatively high sampling rate, is a perfect tool for application in direct, eddy covariance, but when more than one m/z are monitored sequentially the timeseries are not continuous any more, but disjunct. As typically several compounds are selected, the instrument can serve as a disjunct sampler, such that the quadrupole analyses one m/z after another during continuous flow. Its use in this manner has been termed ‘virtual disjunct eddy covariance’ (vDEC) (Karl, 2002) or ‘continuous flow disjunct eddy covariance’ (cfDEC) (Rinne et al., 2008; Rinne et al., 2002); both names denote the same approach. Files containing 25-min arrays of wind and PTR-MS data were validated for periods of breakdown or other disturbances according to the log file. After a careful examination, no raw data files have been marked for despiking or detrending. Double coordinate rotation has been applied to the wind speed vectors in order to account for tilts of the anemometer. Each data row corresponding to a given VOC was converted to ppbv (as described in Sect. SI-3) and subsequently to $\mu\text{g m}^{-3}$ using instantaneous pressure values from the Vaisala sensor attached close to the sonic anemometer. For PTR-MS and wind data, the gaps between PTR-MS rows

were filled with “NaN”s in order to align the frequency of the two time series, and the covariance function was then obtained by computing separately for each VOC the covariance between the instantaneous deviation in mixing ratio (χ') and the instantaneous deviation in vertical wind velocity (w') (i.e., $\text{cov}\langle w'\chi' \rangle$) for each time lag step (0.05 s) expressed as a shift in the wind row versus concentration row. If a clear maximum in the covariance was found within the time lag window, which was defined as at least twice the theoretical lag time and not less than twice the cycle length, then the time lag was recorded for this 25 min period and applied in the final computation of the flux as below:

$$F_{VOC} = \sum (w_i - \bar{w}) \times (\chi_{i+\tau} - \bar{\chi}) \quad (\text{S3})$$

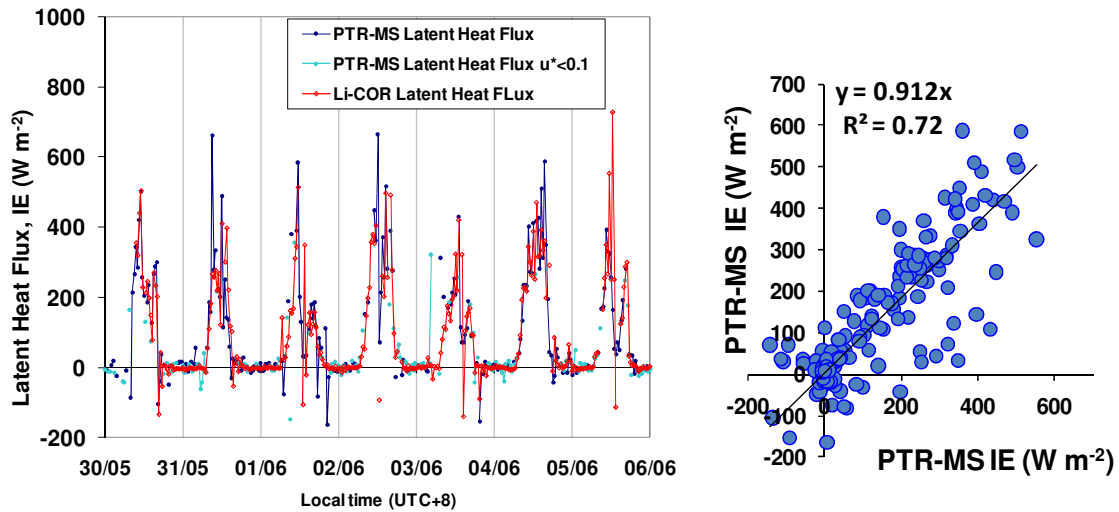
where w_i and \bar{w} are the instantaneous value and mean over an integration period, respectively, for vertical wind velocity, $\chi_{i+\tau}$ is the lag-time adjusted instantaneous value for the mixing ratio and $\bar{\chi}$ is the mean mixing ratio over the same integration period.

The optimum time lag was found automatically from the maximum covariance using a LabVIEW program. If no acceptable maximum was found, or if the flux value was below the detection limit (defined as 3 times the standard deviation of the covariance for lag times well outside the possible window (Spirig et al., 2005), then the data point was marked as invalid and was not included in further analysis. Finally, the accepted lag times were manually examined in terms of their variability. If the lag time exceeded the theoretical lag time (based on sample flow rates) by more than the length of a measurement cycle, or if the lag time found from the covariance functions of shorter integration time sub-periods (e.g. 5 min) was found variable within the 25 min period, then any peak in the covariance found by the program was marked unreal (pseudopeak). However, the lag time value was allowed to be variable by not more than 30% within a 25-min period (as found on 5-min integration times).

In addition, the data were labelled according to routine tests commonly used in eddy covariance for filtering purposes (Clement et al., 2009; Foken and Wichura, 1996; Langford et al., 2009a; Moncrieff et al., 1997): the lower limit for the friction velocity was normally set to 0.15 m s^{-1} and points below this threshold were not included in analyses unless for specific tests. According to the FLUXNET criteria for ideal conditions described by Foken et al. (2004) the turbulence was quite well developed at the site, with 90 % of data in the first 3

1 classes and no data ranked in 8th or 9th category. However, at night, friction velocities were
2 typically below the threshold of 0.15 m s⁻¹. According to the recommendations of Foken and
3 Wichura (1996), data were not included in further analysis if the deviation from the ideal
4 integral similarity characteristics was higher than 60%, and were labelled lower quality if they
5 were within 30-60% of the ideal. A stationarity test (the value for the flux integrated over 25
6 min compared with the average of 5 values of fluxes integrated over 5 min segments of the
7 same averaging period) was used to exclude non-stationary data when the difference was
8 above 60% and to label as low quality periods with differences between 30 and 60%. These
9 tests were done on the sensible heat data and the affected periods were also removed from the
10 VOC flux datasets.

11 Flux losses associated with signal damping due to residence time in the tubing were assessed
12 by comparing latent heat fluxes derived from m/z 37, calibrated using specific humidity
13 converted from relative humidity (Vaisala WXT Weather Transmitter), with latent heat fluxes
14 from the an open path gas analyser (LI-COR 7500 Infrared Gas Analyser; (Skiba et al.,
15 2011)). The close agreement (Figure S3) suggested that flux losses due to damping in the
16 PTR-MS inlet line and due to the internal 1 Hz response time of the PTR-MS were negligible.



17
18 Figure S3. Comparison of latent heat fluxes (IE) derived by PTR-MS and open-path infrared gas
19 analyser: a) time series b) linear regression.

20

21 Finally, low frequency losses were examined by comparison with fluxes with longer
22 averaging periods (Langford et al., 2009a) and the error introduced by disjunct sampling was

estimated by comparing disjunct series for sensible heat flux (corresponding to times when PTR-MS data were available) with continuous data for sensible heat flux (Langford et al., 2009b). The overall flux losses were found to be below 10% and no corrections have been made. Taking all above into account an average 35 % precision for the flux was estimated.

SI-6 Distributions of mixing ratios

Figure S4 shows the frequency distributions of the mixing ratios for the individual VOCs observed over the oil palm plantation.

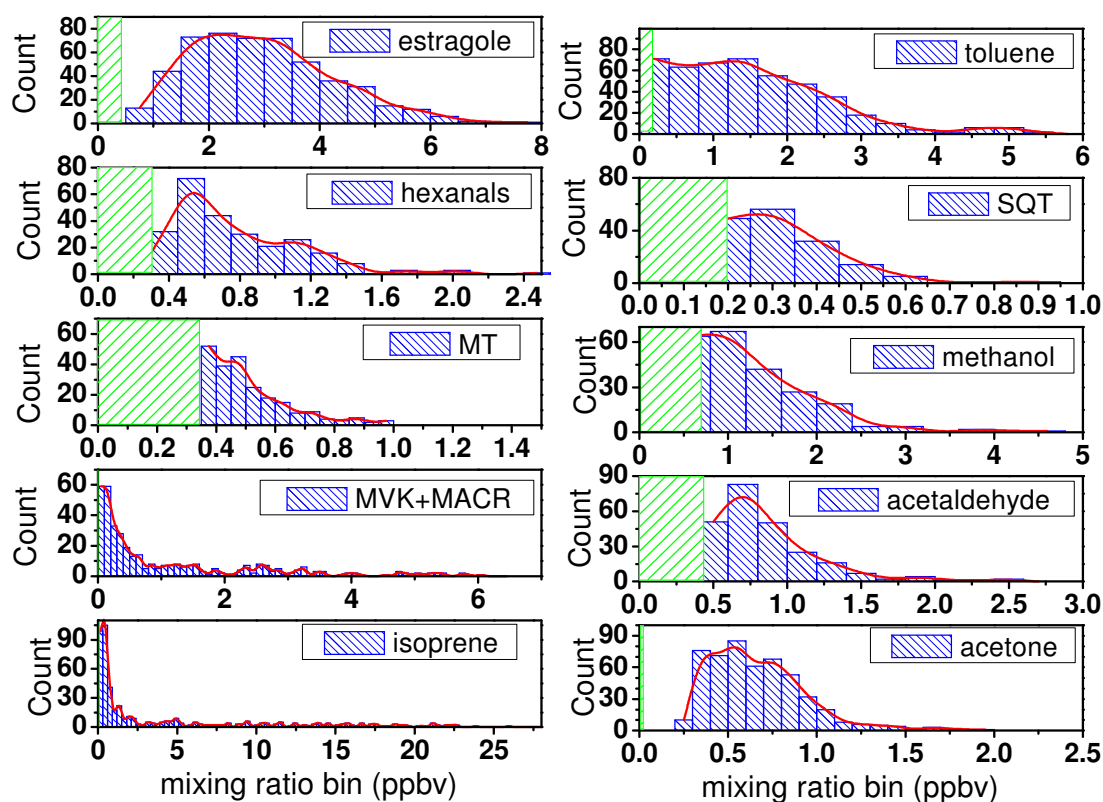


Figure S4. Distributions of the volume mixing ratio values of the compounds measured in the flux mode. Green areas correspond to detection limits.

SI-7 Possible isoprene hydroxyhydroperoxides and epoxides

Figure S5 shows the approximate mixing ratio of the sum of isoprene peroxides and epoxides as derived from m/z 101.

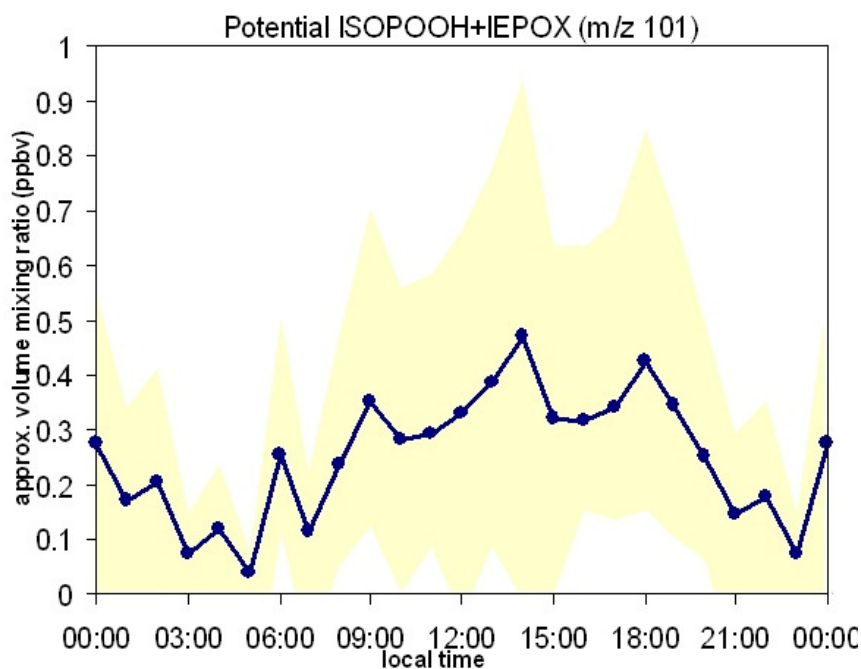


Figure S5. Possible isoprene peroxides and epoxides coinciding at 101 m/z ion channel.

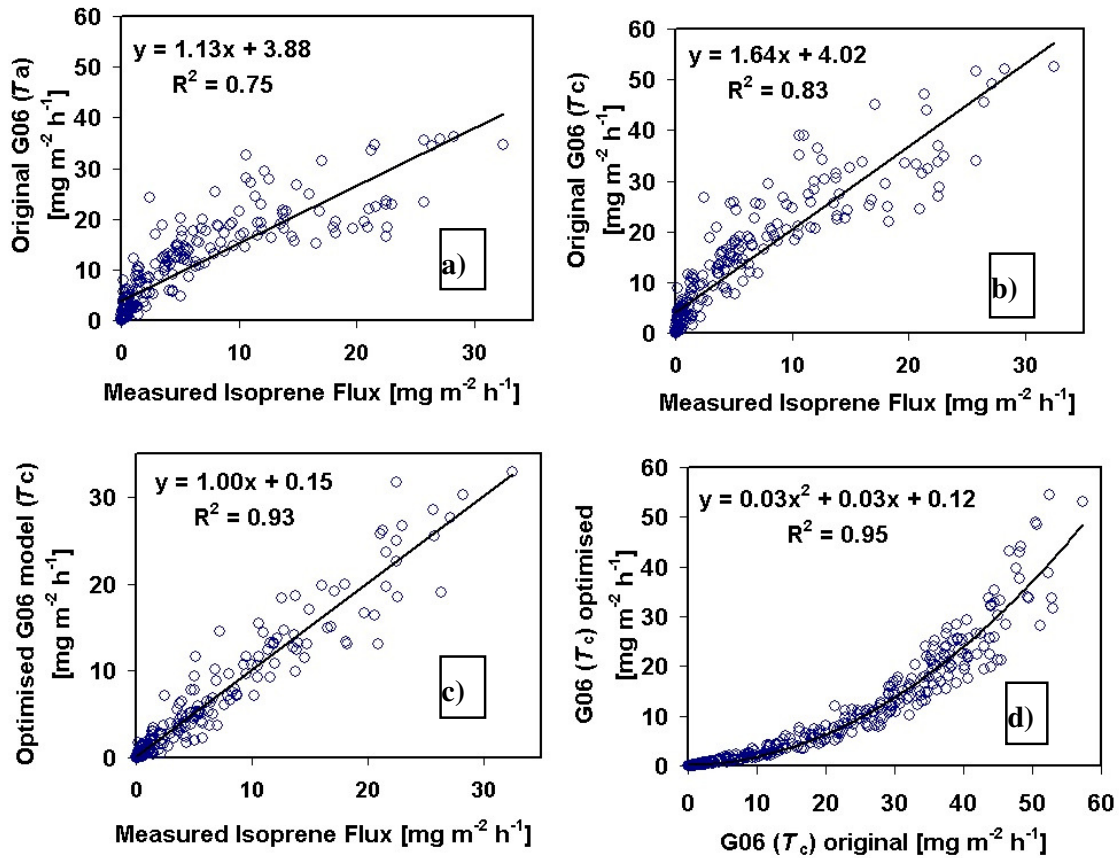
SI-8 Comparisons between parameterised and original G06 model

The Guenther et al. (2006) model (G06) is the most advanced empirical model for terpene emission, which is a significant advancement from previous Guenther et al. models (e.g. Guenther et al., 1995) in that the parameters which used to assume constant values (i.e., α , C_p , T_{opt} and E_{opt}) were extended to simulate variations in enzymatic kinetics and isoprene substrate availability, caused by previous history of temperature and PAR, as tested in a range of field studies (Geron et al., 2000; Hanson and Sharkey, 2001; Monson et al., 1994; Petron et al., 2001; Sharkey et al., 1999). Ten empirical parameters have been chosen and labelled analogously to those in equations presented for estragole emission parameterisation by Misztal et al. (2010). These equations for the temperature and PAR dependent activity factors (γ_T and γ_P) were merged together into one equation so the parameterised flux is represented as below Eq. (S4) with the 10 parameters marked as b1-b6, Tb, P0, CT1 and CT2 to be optimised to fit the experimental data from oil palms. The dependent variables were the photosynthetically active radiation (PAR) and the canopy temperature (T) estimated from an ambient temperature using the resistance approach. The P24 and T24 are the 24 h averages of previous PAR and T, respectively; and P240 and T240 are the previous 10-day averages.

$$F_{G06} = \underbrace{\text{BER} \cdot b_3 \cdot \exp[b_2 \cdot (P_{24} - P_0)] \cdot (P_{240})^{0.6} \cdot \frac{[b_1 - b_2 \ln(P_{240})] \cdot \text{PAR}}{\sqrt{1 + [b_1 - b_2 \ln(P_{240})]^2 \cdot \text{PAR}^2}}}_{\gamma_P} \cdot \underbrace{b_5 \cdot \exp[b_6 \cdot (T_{24} - 297)] \cdot \exp[b_6 \cdot (T_{240} - 297)] \cdot \frac{C_{T2} \cdot \exp\left[C_{T1} \cdot \left(\frac{1}{T_{\text{opt}}} - \frac{1}{T}\right) \cdot \frac{1}{0.00831}\right]}{C_{T2} - C_{T1} \cdot \left[1 - \exp\left(C_{T2} \cdot \left(\frac{1}{T_{\text{opt}}} - \frac{1}{T}\right) \cdot \frac{1}{0.00831}\right)\right]}}_{\gamma_T} \quad (\text{S4})$$

1
2 Comparison between the original G06 model using $T_a(15 \text{ m})$, measured 3 m above the
3 canopy, and the measurement is presented in Figure S6a, and the analogous comparison using
4 the canopy temperature (T_c) in the G06 model in Figure S6b. By optimising the G06
5 parameters based on the measured canopy flux, the model fit improves significantly from
6 originally $r^2 = 0.75$ to 0.91, if a constant basal emission rate (BER) and $T_a(15 \text{ m})$ are used (not
7 shown). Replacing $T_a(15 \text{ m})$ for T_c in the original model increases the coefficient of
8 determination to 0.83 (Figure S6b) which after parameter adjustment improves further to 0.93
9 (Figure S6c). The corresponding time series are almost identical. The comparison of the
10 original and the parameterised G06 model outputs for oil palms has a quadratic relationship
11 (Figure S6d), which suggests that the original model underestimates the emission at moderate
12 temperatures and light levels. For the adjusted BER, the original G06 has a tendency to
13 overestimate the small flux region (morning, afternoon) while underestimating the high fluxes
14 (noon) in comparison with the 1:1 slope with measurement.

15



1

2 Figure S6 Comparison of measured fluxes with the original G06 using ambient temperature at a
 3 constant BER of $12.8 \text{ mg m}^{-2} \text{ h}^{-1}$ (a), with the original G06 using canopy temperature at a constant
 4 BER of $12.8 \text{ mg m}^{-2} \text{ h}^{-1}$ (b), and the parameterised G06 optimised for oil palm plantation using canopy
 5 temperature at a constant BER of $22.8 \text{ mg m}^{-2} \text{ h}^{-1}$ (c). The relationship between original and optimised
 6 G06 model is shown in (d).

7 SI-9 Isoprene response to PAR

8 Figure S7 shows isoprene emission in response to PAR derived from PTR-MS canopy
 9 measurements. The curve is getting much steeper after $1000 \mu\text{mol m}^{-2} \text{ s}^{-1}$. The relationship
 10 with temperature was presented in the main text.(Figure 7)

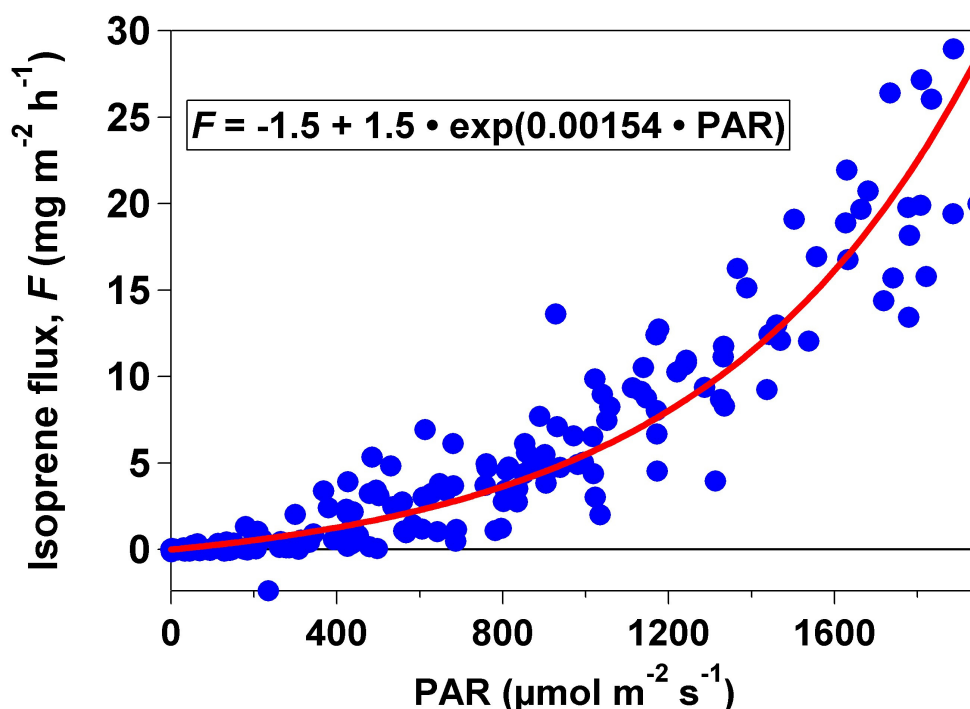


Figure S7. Relationship between isoprene flux measured above oil palm canopy and PAR.

References

- Clement, R. J., Burba, G. G., Grelle, A., Anderson, D. J., and Moncrieff, J. B.: Improved trace gas flux estimation through IRGA sampling optimization, *Agricultural and Forest Meteorology*, 149, 623-638, 10.1016/j.agrformet.2008.10.008, 2009.
- Davison, B., Taipale, R., Langford, B., Misztal, P., Fares, S., Matteucci, G., Loreto, F., Cape, J. N., Rinne, J., and Hewitt, C. N.: Concentrations and fluxes of biogenic volatile organic compounds above a Mediterranean macchia ecosystem in western Italy, *Biogeosciences*, 6, 1655-1670, 2009.
- Foken, T., and Wichura, B.: Tools for quality assessment of surface-based flux measurements, *Agricultural and Forest Meteorology*, 78, 83-105, 1996.
- Foken, T., Göckede, M., Mauder, M., Mahrt, L., Amiro, B., and Munger, W.: Post-field data quality control, in: *Handbook of Micrometeorology: A guide for surface flux measurement and analysis.*, edited by: Lee, W. M. X., and Law, B., Kluwer Academic Publishers, Dordrecht, 181-203, 2004.
- Geron, C., Guenther, A., Sharkey, T., and Arnts, R. R.: Temporal variability in basal isoprene emission factor, *Tree Physiology*, 20, 799-805, 2000.
- Guenther, A., Hewitt, C. N., Erickson, D., Fall, R., Geron, C., Graedel, T., Harley, P., Klinger, L., Lerdau, M., McKay, W. A., Pierce, T., Scholes, B., Steinbrecher, R., Tallamraju, R., Taylor, J., and Zimmerman, P.: A global-model of natural volatile organic-compound emissions, *Journal of Geophysical Research-Atmospheres*, 100, 8873-8892, 1995.

1 Guenther, A., Karl, T., Harley, P., Wiedinmyer, C., Palmer, P. I., and Geron, C.: Estimates of
2 global terrestrial isoprene emissions using MEGAN (Model of Emissions of Gases and
3 Aerosols from Nature), *Atmos. Chem. Phys. Discuss.*, 6, 107-173, 2006.

4 Hanson, D. T., and Sharkey, T. D.: Rate of acclimation of the capacity for isoprene emission
5 in response to light and temperature, *Plant Cell and Environment*, 24, 937-946, 2001.

6 Helsel, D. R.: Less than obvious - statistical treatment of data below the detection limit,
7 *Environmental Science & Technology*, 24, 1766-1774, 1990.

8 Karl, T. G., C. Spirig, et al.: Virtual disjunct eddy covariance measurements of organic
9 compound fluxes from a subalpine forest using proton transfer reaction mass spectrometry,
10 *Atmospheric Chemistry and Physics*, 2, 279-291, 2002.

11 Kim, S., Karl, T., Helmig, D., Daly, R., Rasmussen, R., and Guenther, A.: Measurement of
12 atmospheric sesquiterpenes by proton transfer reaction-mass spectrometry (PTR-MS), *Atmos.*
13 *Meas. Tech.*, 2, 99-112, 2009.

14 Kuhn, U., Andreae, M. O., Ammann, C., Araujo, A. C., Brancaleoni, E., Ciccioli, P., Dindorf,
15 T., Frattoni, M., Gatti, L. V., Ganzeveld, L., Kruijt, B., Lelieveld, J., Lloyd, J., Meixner, F.
16 X., Nobre, A. D., Poschl, U., Spirig, C., Stefani, P., Thielmann, A., Valentini, R., and
17 Kesselmeier, J.: Isoprene and monoterpene fluxes from Central Amazonian rainforest inferred
18 from tower-based and airborne measurements, and implications on the atmospheric chemistry
19 and the local carbon budget, *Atmospheric Chemistry and Physics*, 7, 2855-2879, 2007.

20 Langford, B., Davison, B., Nemitz, E., and Hewitt, C. N.: Mixing ratios and eddy covariance
21 flux measurements of volatile organic compounds from an urban canopy (Manchester, UK),
22 *Atmos. Chem. Phys.*, 9, 1971-1987, 2009a.

23 Langford, B., Nemitz, E., House, E., Phillips, G. J., Famulari, D., Davison, B., Hopkins, J. R.,
24 Lewis, A. C., and Hewitt, C. N.: Fluxes and concentrations of volatile organic compounds
25 above central London, UK, *Atmos. Chem. Phys. Discuss.*, 9, 17297-17333, 2009b.

26 Misztal, P. K., Owen, S. M., Guenther, A. B., Rasmussen, R., Geron, C., Harley, P., Phillips,
27 G. J., Ryan, A., Edwards, D. P., Hewitt, C. N., Nemitz, E., Siong, J., Heal, M. R., and Cape, J.
28 N.: Large estragole fluxes from oil palms in Borneo, *Atmos. Chem. Phys.*, 10, 4343-4358,
29 10.5194/acp-10-4343-2010, 2010.

30 Moncrieff, J., Valentini, R., Greco, S., Guenther, S., and Ciccioli, P.: Trace gas exchange over
31 terrestrial ecosystems: methods and perspectives in micrometeorology, *J. Exp. Bot.*, 48, 1133-
32 1142, 10.1093/jxb/48.5.1133, 1997.

33 Monson, R. K., Harley, P. C., Litvak, M. E., Wildermuth, M., Guenther, A. B., Zimmerman,
34 P. R., and Fall, R.: Environmental and developmental controls over the seasonal pattern of
35 isoprene emission from aspen leaves, *Oecologia*, 99, 260-270, 1994.

36 Nemitz, E., Loubet, B., Lehmann, B. E., Cellier, P., Neftel, A., Jones, S. K., Hensen, A., Ihly,
37 B., Tarakanov, S. V., and Sutton, M. A.: Turbulence characteristics in grassland canopies and
38 implications for tracer transport, *Biogeosciences*, 6, 1519-1537, 2009.

39 Petron, G., Harley, P., Greenberg, J., and Guenther, A.: Seasonal temperature variations
40 influence isoprene emission, *Geophysical Research Letters*, 28, 1707-1710, 2001.

41 Rinne, J., Durand, P., and Guenther, A.: An airborne disjunct eddy covariance system:
42 Sampling strategy and instrument design, 15th Symposium on Boundary Layers and
43 Turbulence, 151-154, 2002.

1 Rinne, J., Douffet, T., Prigent, Y., and Durand, P.: Field comparison of disjunct and
2 conventional eddy covariance techniques for trace gas flux measurements, *Environmental*
3 *Pollution*, 152, 630-635, 2008.

4 Sharkey, T. D., Singsaas, E. L., Lerdau, M. T., and Geron, C. D.: Weather effects on isoprene
5 emission capacity and applications in emissions algorithms, *Ecological Applications*, 9, 1132-
6 1137, 1999.

7 Skiba, U. M., Siong, J., Helfter, C., Di Marco, C., Linatoc, A., Fowler, D., and Nemitz, E.:
8 Greenhouse gas (N₂O, CH₄ and CO₂) exchange with contrasting land uses in SE Asia,
9 *Atmos. Chem. Phys. Discuss.*, in preparation for submission, 2011.

10 Spirig, C., Neftel, A., Ammann, C., Dommen, J., Grabmer, W., Thielmann, A., Schaub, A.,
11 Beauchamp, J., Wisthaler, A., and Hansel, A.: Eddy covariance flux measurements of
12 biogenic VOCs during ECHO 2003 using proton transfer reaction mass spectrometry,
13 *Atmospheric Chemistry and Physics*, 5, 465-481, 2005.

14 Steinbacher, M., Dommen, J., Ammann, C., Spirig, C., Neftel, A., and Prevot, A. S. H.:
15 Performance characteristics of a proton-transfer-reaction mass spectrometer (PTR-MS)
16 derived from laboratory and field measurements, *International Journal of Mass Spectrometry*,
17 239, 117-128, 2004.

18 Taipale, R., Ruuskanen, T. M., Rinne, J., Kajos, M. K., Hakola, H., Pohja, T., and Kulmala,
19 M.: Technical Note: Quantitative long-term measurements of VOC concentrations by PTR-
20 MS - measurement, calibration, and volume mixing ratio calculation methods, *Atmospheric*
21 *Chemistry and Physics*, 8, 6681-6698, 2008.

22 Tani, A., Hayward, S., and Hewitt, C. N.: Measurement of monoterpenes and related
23 compounds by proton transfer reaction-mass spectrometry (PTR-MS), *International Journal of*
24 *Mass Spectrometry*, 223, 561-578, 2003.

25 Tani, A., Hayward, S., Hansel, A., and Hewitt, C. N.: Effect of water vapour pressure on
26 monoterpene measurements using proton transfer reaction-mass spectrometry (PTR-MS),
27 *International Journal of Mass Spectrometry*, 239, 161-169, 2004.

28 Warneke, C., van der Veen, C., Luxembourg, S., de Gouw, J. A., and Kok, A.: Measurements
29 of benzene and toluene in ambient air using proton-transfer-reaction mass spectrometry:
30 calibration, humidity dependence, and field intercomparison, *International Journal of Mass*
31 *Spectrometry*, 207, 167-182, 2001.

32 Zhao, J., and Zhang, R.: Proton transfer reaction rate constants between hydronium ion
33 (H₃O⁺) and volatile organic compounds, *Atmospheric Environment*, 38, 2177-2185, 2004.

34

35